Electrostatic Interactions Guide the Active Site Face of a Structure-Specific Ribonuclease to Its RNA Substrate[†]

Matthew J. Plantinga,[‡,§,||] Alexei V. Korennykh,[⊥,@,#] Joseph A. Piccirilli,*[,‡,⊥,@] and Carl C. Correll*[,‡,§,||]

Department of Biochemistry and Molecular Biology, Department of Chemistry, and Howard Hughes Medical Institute, The University of Chicago, Chicago, Illinois 60637, and Department of Biochemistry and Molecular Biology, Rosalind Franklin University of Medicine and Science, North Chicago, Illinois 60064

Received April 4, 2008; Revised Manuscript Received June 20, 2008

ABSTRACT: Restrictocin, a member of the α-sarcin family of site-specific endoribonucleases, uses electrostatic interactions to bind to the ribosome and to RNA oligonucleotides, including the minimal specific substrate, the sarcin/ricin loop (SRL) of 23S−28S rRNA. Restrictocin binds to the SRL by forming a ground-state E:S complex that is stabilized predominantly by Coulomb interactions and depends on neither the sequence nor structure of the RNA, suggesting a nonspecific complex. The 22 cationic residues of restrictocin are dispersed throughout this protein surface, complicating a priori identification of a Coulomb interacting surface. Structural studies have identified an enzyme−substrate interface, which is expected to overlap with the electrostatic E:S interface. Here, we identified restrictocin residues that contribute to binding in the E:S complex by determining the salt dependence [$\partial \log(k_2/K_{1/2})/\partial \log[\mathrm{KCl}]$] of cleavage of the minimal SRL substrate for eight point mutants within the protein designed to disrupt contacts in the crystallographically defined interface. Relative to the wild-type salt dependence of −4.1, a subset of the mutants clustering near the active site shows significant changes in salt dependence, with differences of magnitude being ≥0.4. This same subset was identified using calculated salt dependencies for each mutant derived from solutions to the nonlinear Poisson−Boltzmann equation. Our findings support a mechanism in which specific residues on the active site face of restrictocin (primarily K110, K111, and K113) contribute to formation of the E:S complex, thereby positioning the SRL substrate for site-specific cleavage. The same restrictocin residues are expected to facilitate targeting of the SRL on the surface of the ribosome.

Coulomb interactions between cationic protein residues and the anionic phosphodiester backbone of RNA and DNA facilitate binding of many proteins to nucleic acids. Such interactions give rise to the characteristic salt dependencies of binding, which change upon mutation of the participating protein residues (*1–3*). Tracking salt dependencies thus provides a powerful approach by which to identify residues involved in protein−nucleic acid recognition. There is a paucity of relevant studies for RNA−protein interactions because of the dual requirement for structural studies that identify candidate surface contacts and solution studies that pinpoint functionally important contacts and evaluate their contribution. The site-specific ribotoxin restrictocin is an ideal candidate for study because it exploits electrostatic interactions for activity (*4*) and it is sufficiently well characterized structurally (*5, 6*) and kinetically (*7*).

The cationic ribotoxin restrictocin is a member of the α-sarcin family of fungal ribotoxins that target the conserved sarcin/ricin loop (SRL)[1] in 23S−28S rRNA (reviewed in refs *8* and *9*). Cleavage of a single bond within the SRL disrupts binding of elongation factors to the ribosome, halts protein synthesis, and ultimately triggers apoptotic cell death (*10*). Structural and functional studies have been aided by the use of minimal RNA oligonucleotide substrates that contain the SRL sequence and undergo site-specific cleavage by the ribotoxins. The SRL folds into two motifs: a GAGA tetraloop and a bulged G motif (*11–14*). Both motifs contribute to ribotoxin recognition (*7, 15*), and cleavage occurs within the tetraloop.

Wool and colleagues demonstrated that salt inhibits both specific cleavage of the ribosome and nonspecific cleavage of poly(A) by α-sarcin (86% identical to restrictocin in sequence) (*16*). To explore the nature of this electrostatic effect, the salt dependence of restrictocin was determined using eq 1 (*4*):

$$n = \partial \log(k_2/K_{1/2})/\partial \log[\mathrm{KCl}] \quad (1)$$

[†] This work was supported by grants to C.C.C. from the National Institutes of Health (GM59872) and to J.A.P. from the Howard Hughes Medical Institute.

* To whom correspondence should be addressed. C.C.C.: Department of Biochemistry and Molecular Biology, Rosalind Franklin University of Medicine and Science, North Chicago, IL 60064. Telephone: (847) 578-8611. Fax: (847) 578-3240. E-mail: carl.correll@rosalindfranklin.edu. J.A.P. Phone (773)702-9312; fax (773)702-0271; e-mail: jpicciri@uchicago.edu.

[‡] Department of Biochemistry and Molecular Biology, The University of Chicago.

[§] Rosalind Franklin University of Medicine and Science.

[||] Present address: Department of Biochemistry and Molecular Biology, Rosalind Franklin University of Medicine and Science, North Chicago, IL 60064.

[⊥] Department of Chemistry, The University of Chicago.

[@] Howard Hughes Medical Institute, The University of Chicago.

[#] Present address: Department of Biochemistry and Biophysics, University of California, San Francisco, CA 94158.

[1] Abbreviations: NLPB, nonlinear Poisson−Boltzmann; SRL, sarcin/ricin loop.

10.1021/bi800592g CCC: $40.75
Published on Web 08/02/2008

Scheme 1

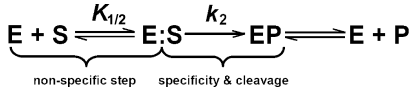

where the kinetic parameter $k_2/K_{1/2}$ [the single-turnover equivalent of k_{cat}/K_M (Scheme 1)] replaces the more commonly used $1/K_D$ (*1*). For restrictocin, $K_{1/2}$ but not k_2 is affected by salt concentration, and the values of $K_{1/2}$ are equal to K_D (*7*). Thus, salt-dependent changes in $k_2/K_{1/2}$ reflect changes in binding of the RNA to the enzyme to form the ground-state complex (E:S), specifically, changes to $1/K_D$. The salt-independent parameter k_2 reports on subsequent specific recognition and cleavage of the SRL. Similar kinetic measurements were used previously during studies of RNase A, where the salt dependence of substrate binding and k_{cat}/K_M correlated closely (*2*).

Cleavage of the minimal SRL substrate by restrictocin is salt-dependent ($n = -4.1$), consistent with electrostatic forces providing a major contribution to enzyme−substrate binding (*4*). Unexpectedly, the stability of the resulting complex appears to have little dependence on nucleotide sequence or structure. All nucleic acid substrates tested that were at least 25 nucleotides in length bound to restrictocin with the same affinity as the SRL. These findings suggest that nonspecific electrostatic interactions drive the formation of the enzyme−substrate complex (designated herein as E:S). An ensemble of different RNA−protein complexes best represents the nonspecific nature of these electrostatic interactions.

Cocrystal structural studies of restrictocin bound to substrate analogues identify one enzyme−substrate interface (*6*). The number of observed salt bridges between cationic residues and RNA phosphates (between one and three depending on the structure used) qualitatively agrees with the salt dependence data; however, it is unclear whether the crystallographically defined contacts reflect those found in the ensemble of E:S complexes, given the lack of substrate specificity in this complex. Moreover, there is no indication of which residues contribute to the Coulomb interactions in the E:S complex because the 22 cationic residues of the 149-amino acid restrictocin are dispersed throughout its surface. However, due to the requirement for subsequent substrate docking into the active site, the E:S interface is expected to overlap with that observed in the crystal structures.

To begin exploring the contribution of surface residues to substrate binding, we mutated three cationic residues located outside the crystallographic SRL−restrictocin interface to aspartate: R21, K28, and R63. R63 is located near the edge of the interface, whereas R21 and K28 are located on the opposite face of the protein (*4*). Negligible effects on $k_2/K_{1/2}$ for the SRL substrate were observed for K63D, R21D/K28D, and R21D/K28D/K63D. Additionally, the R21D/K28D/K63D triple mutant had the same salt dependence (n) as wild-type restrictocin for SRL cleavage but had a reduced salt dependence for cleavage of the ribosome. These data raise the possibility that restrictocin forms the electrostatic E:S complex in an oriented fashion, using residues on the active site face to interact with the substrate.

To test this hypothesis, we identified residues that contribute to binding in the electrostatic E:S complex by determining the salt dependence for eight mutants designed to disrupt interface contacts. Five mutants within the RNA−protein interface show a significant change in salt dependence, demonstrating that these residues make electrostatic contributions to formation of the E:S complex. Mutation of residues outside the interface exhibited no change in salt dependence (*4*). These findings support the view that restrictocin uses residues on its active site face to form electrostatic contacts to the SRL substrate in the initial E:S complex.

MATERIALS AND METHODS

Expression and Purification of Restrictocin. The restrictocin gene from *Aspergillus restrictus* was cloned into the periplasmic expression vector pEH-T1 (gift of C. N. Pace, Texas A&M University, College Station, TX) to create pREST. Amino acid substitution mutants were created via site-directed mutagenesis of pREST. Proteins were expressed and purified as described previously (*7*) with the following change: SP Sepharose FF cation exchange resin (Amersham) was used in 15 mM MES (pH 6.0). Proteins were stored at 4 °C in 10−15 mM Tris (pH 7.5) at concentrations of ≥2 μM.

Selection of Residues for Mutation. Three structures were used to identify residues located within the RNA−protein interface (*6*): the "bound" structure (PDB entry 1JBS), which shows sequence-specific contacts to the bulged G motif; the "misdocked" structure (PDB entry 1JBR), which shows substrate contacts within the active site; and a model of a "correctly docked" complex, which incorporates elements of both the bound and misdocked structures.

Kinetics Measurements. SRL RNA was synthesized by Dharmacon and purified by nondenaturing 20% PAGE. Reactions were performed as described previously (*4*). The salt dependence, n, for each mutant is the slope of a plot of $\log(k_2/K_{1/2})$ versus log[KCl] (eq 1). For each mutant, error values for n are the standard deviation of at least three independent determinations of n. For Δn values that arose from a difference between two mean values of n, significance was tested at the 99% confidence level using a Student's t test.

Electrostatic Calculations. Numerical solutions to the nonlinear Poisson−Boltzmann equation were determined using APBS (*17*). Atomic charges were assigned with PDB2PQR (*18*) using the AMBER force field (*19*). Protonation states were assigned at pH 7.5 using PROPKA (*20*). The protein and RNA molecules were assigned a low dielectric constant of 2.0 with a solvent dielectric constant of 78.0. Ionic radii of 3.3 Å were used, corresponding to the radius of a hydrated potassium ion. The multigrid solution used a grid size of 161 × 161 × 161 and a solvent radius of 1.6 Å. Binding energies for each RNA−protein complex are the differences between the calculated electrostatic energies of the individual molecules and that of the bound complex. Calculation of the complex energy (E, kilojoules per mole) at multiple salt concentrations ranging from 40 to 100 mM enabled subsequent determination of the salt dependence from a plot of $-E/RT$ versus the natural logarithm of the salt concentration, where $T = 310$ K.

RESULTS

To identify residues that contribute to formation of the E:S complex, we created eight mutants of residues within

Table 1: KCl Dependence of SRL Cleavage by Restrictocin[a]

	n[b]	Δn[c]
wild type	−4.1 ± 0.1	(0)
D40A	−4.6 ± 0.1	−0.5 ± 0.1
K42A	−3.7 ± 0.1	0.4 ± 0.1
Y47F	−4.1	0
H49A	−3.8	0.3
K110A	−3.3 ± 0.3	0.8 ± 0.3
K111A	−3.4 ± 0.2	0.7 ± 0.2
K113A	−3.2 ± 0.2	0.9 ± 0.2
D143A	−4.2	−0.1
R21D/K28D/R63D[d]	−3.9	0.3

[a] Reaction conditions: 10 mM Tris (pH 7.4), 0.05% Triton X-100, $E_0 \sim 1$ nM to 46 μM, [KCl] ~ 12−100 mM. [b] n is the slope of the log linear region on a plot of $\log(k_2/K_{1/2})$ vs log[KCl], where $k_2/K_{1/2}$ reflects specific cleavage only; values are averages of at least three determinations. [c] $\Delta n = n_{Wt} - n_{Mut}$; the error is the propagated subtraction error. [d] From ref *4*.

the crystallographically determined RNA−protein interface (Materials and Methods): D40A, K42A, Y47F, H49A, K110A, K111A, K113A, and D143A. The anionic residues form direct and solvent-mediated substrate contacts. D40 forms an outer sphere coordination to a potassium ion located in the tetraloop of the SRL. D143 is the only other anionic residue that interacts with the substrate in any of the available structures. Cationic residues K42, K110, K111, and K113 form contacts to the SRL. K110 and K111 form salt bridges to phosphate oxygen atoms of the SRL RNA (>3.4 Å). Given its location, K42 is also expected to form a strong electrostatic interaction with the backbone (3.7 Å). In contrast, K113 is expected to form longer-range electrostatic interactions (~6.6 Å). K110, K111, and K113 form contacts to the bulged G motif, with K113 forming sequence-specific contacts to the bulged G. Y47 and H49 are in the active site. H49 is expected to carry a partial positive charge because its measured pK_a of 7.7 in the presence of a dinucleotide substrate (*21*) is similar to the pH of 7.5 that was used in the assays. In contrast, Y47 is not charged and serves as a control.

To test if the targeted residues affect formation of the E:S complex, we determined the change in salt dependence for SRL cleavage by mutants at these positions [$\Delta n = n_{Wt} - n_{Mut}$ (Table 1 and Figure 1)]. Cleavage of a ^{32}P-labeled SRL oligonucleotide was performed at 37 °C under $k_2/K_{1/2}$ conditions ($E_0 \ll K_{1/2}$, and $S_0 \ll E_0$) in 10 mM Tris (pH 7.5) containing 0.05% Triton X-100 and 30−100 mM KCl. Other chloride salts show equivalent salt dependence for formation of the E:S complex (NH_4Cl and LiCl; supplementary Figure 2A,B in ref *4*). The salt dependence of each mutant, n, is the slope of a plot of log $k_2/K_{1/2}$ versus log[KCl]; the value of n was then subtracted from that of the wild-type protein to yield the change in salt dependence, Δn, for each mutant. Mutation of a cationic residue that contributes to binding is expected to produce a smaller salt dependence ($\Delta n > 0$) because fewer cationic residues are available to interact with the anionic RNA substrate and therefore displace fewer anions from the RNA surface upon complex formation. Conversely, mutation of an anionic residue that contributes to binding is expected to produce a greater salt dependence ($\Delta n < 0$) because the net increase in positive charge strengthens the interactions with RNA and requires displacement of a greater number of ions from the RNA surface upon binding. Removal of a single protein charge from RNA−protein interfaces produced Δn values of ~0.5 (*22, 23*). Mutation of residues that do not contribute to electrostatic binding is expected to result in little or no change in salt dependence ($\Delta n \sim 0$).

Three lines of evidence suggest that the altered salt dependence upon mutation results from disruption of electrostatic interactions between the RNA and the endonuclease rather than salt-induced structural changes to the endonuclease or RNA in the complex. First, similar salt dependence profiles are observed for both a minimal specific substrate (the SRL) and nonspecific substrates (single-stranded substrates) (*4*), indicating that the observed salt dependence is independent of the RNA structure. Second, as demonstrated herein, the neutral mutation Y47F does not change the salt dependence ($\Delta n = 0$), despite an ~280-fold decrease in k_2 relative to that of the wild-type enzyme. Only mutations of charged residues lead to changes in the salt dependence (see below), suggesting that the salt inhibition reflects disruption of electrostatic interactions rather than structural rearrangements upon formation of the E:S complex. Third, comparison of crystal structures of restrictocin alone or in complex with substrate analogues reveals negligible structural changes in the protein.

It is unlikely that the changes in salt dependence arise from structural changes due to amino acid substitution. As alanine substitutions do not remove backbone atoms, changes to the protein structure are not expected (*24, 25*). Consistent with this notion, replacement of three active site residues with glutamine (H49Q/E95Q/H136Q) was structurally isomorphous (M. J. Plantinga and C. C. Correll, unpublished observations).

Alanine mutants of cationic residues within the RNA−protein interface exhibit a shallower slope in their salt dependence plots (Table 1 and Figure 1). For three of the mutants, Δn approaches unity: K110A has a Δn of 0.8, K111A a Δn of 0.7, and K113A a Δn of 0.9. These residues (designated the lysine triad) cluster to form a highly positive patch in loop 4 (L4, residues 98−118) at the edge of the predicted RNA−protein interface (Figure 1D). In accord with the contribution of these three lysine residues to formation of the electrostatic E:S complex, they form a patch with the highest positive potential (Figure 2A). The other mutants, K42A and H49A, have a smaller effect on salt dependence, with Δn values of 0.4 and 0.3, respectively. K42 is found in loop 2 (L2, residues 36−48), near the lysine triad. H49 is located in the active site; the observed moderate decrease in the salt dependence for the H49A mutant supports the previous finding that this residue carries a partial charge in the ground-state complex (*26*).

For the alanine mutants of anionic residues, D40A shows a steeper slope in the salt dependence plot ($\Delta n = -0.5$) whereas D143A has the same salt dependence as wild-type restrictocin ($\Delta n = -0.1$). D40 is located in L2 near K42 and the lysine triad in L4 (Figure 1D). The change in salt dependence for the D40A mutant is consistent with removal of an anionic residue increasing the net cationic character of the protein and thus strengthening electrostatic interactions with the anionic RNA substrate. In contrast, the lack of a change in the salt dependence for D143A demonstrates that this residue does not contribute electrostatically to formation of the E:S complex, although D143 is located near the active site.

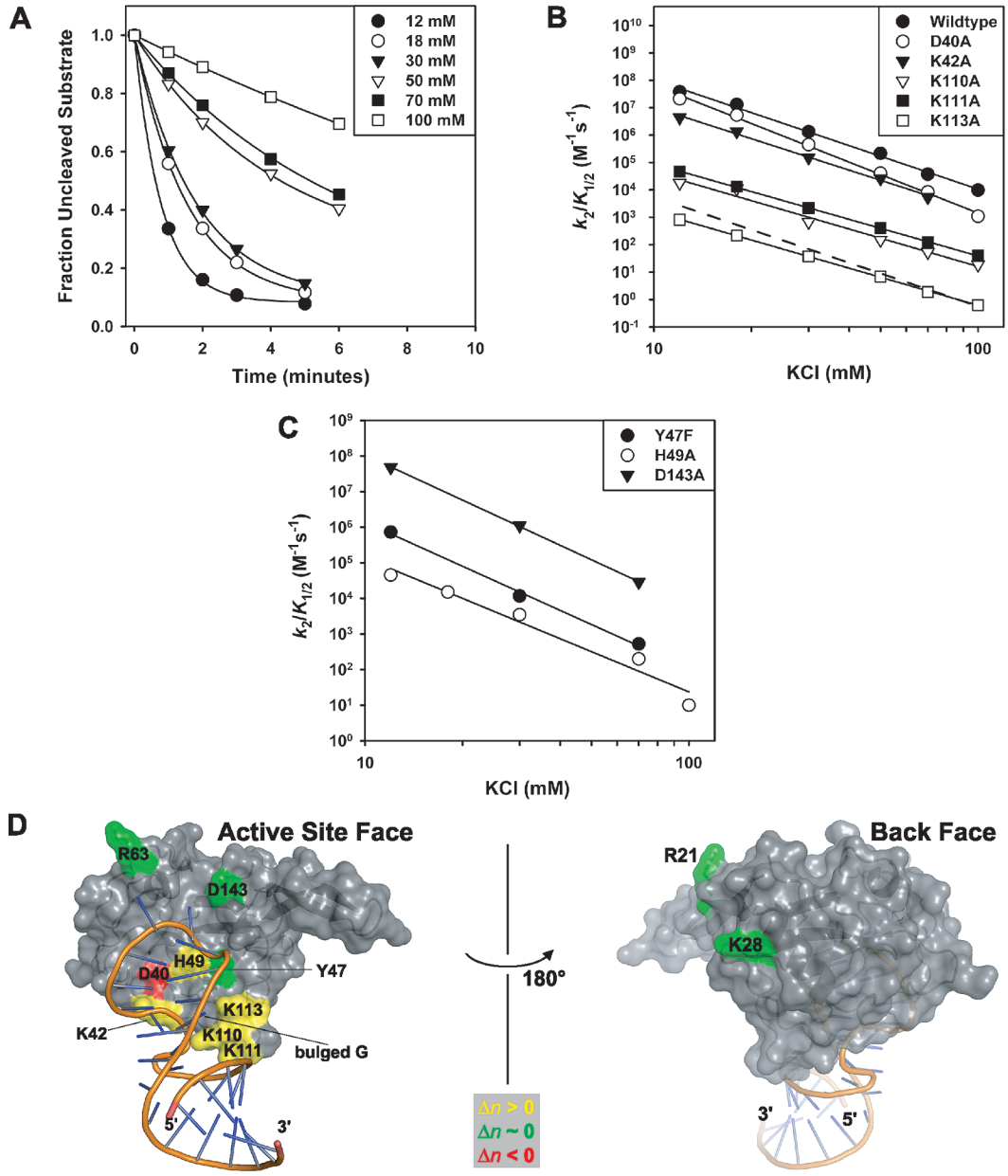

FIGURE 1: Salt dependence of restrictocin mutants. (A) Cleavage of the SRL by D40A at varying salt concentrations ranging from 12 to 100 mM KCl. Reactions were conducted under multiple-turnover conditions at 37 °C in 10 mM Tris (pH 7.4) and 0.05% Triton X-100 containing [^{32}P]SRL and 1−100 nM restrictocin. (B) Representative salt dependence plots for mutants with multiple determinations (Table 1), including data from panel A. To illustrate the change in salt dependence for K113A, a dotted line is shown with the same slope as the WT salt dependence. Reaction conditions were as described for panel A. (C) Salt dependence plots for mutants with single determinations. Reaction conditions were as described for panel A. (D) Surface representation showing charged residues on the active site face (left) and the backside of restrictocin (right), colored by their effect on salt dependence. The salt dependence for the R21D/K28D/R63D mutant of restrictocin was determined previously (*4*).

Our analysis of the salt dependence data for interface and noninterface mutants indicates that only mutations of charged residues located on the active site face exhibit significant changes in salt dependence (Table 1 and Figures 1 and 2). Changes in salt dependence can result from disruption of direct and/or long-range electrostatic interactions. Mutation of residues outside the E:S interface does not alter the salt dependence, indicating that these residues form neither direct nor long-range electrostatic interactions with the substrate. In contrast, residues on the active site face alter the salt dependence when mutated, consistent with direct electrostatic interactions with the RNA substrate. These findings strongly support a model in which restrictocin uses its active site face to bind to its RNA substrate in the E:S complex, thereby facilitating subsequent specific recognition and cleavage.

To test whether formation of the E:S complex can be described by the nonlinear Poisson−Boltzmann (NLPB) model, we calculated salt dependencies for eight mutants (Figure 3 and Materials and Methods). Kinetic studies indicate that the ground-state E:S complex is not a single structure but rather an ensemble that is partially represented by two restrictocin−substrate analogue cocrystal structures (*4*, *6*, *7*). Thus, both structures were used for these calculations. The n_{calc} values correlate well with experimental n values for complexes of point mutants (Figure 3A), and the Δn_{calc} values are independent of the structure used (Figure

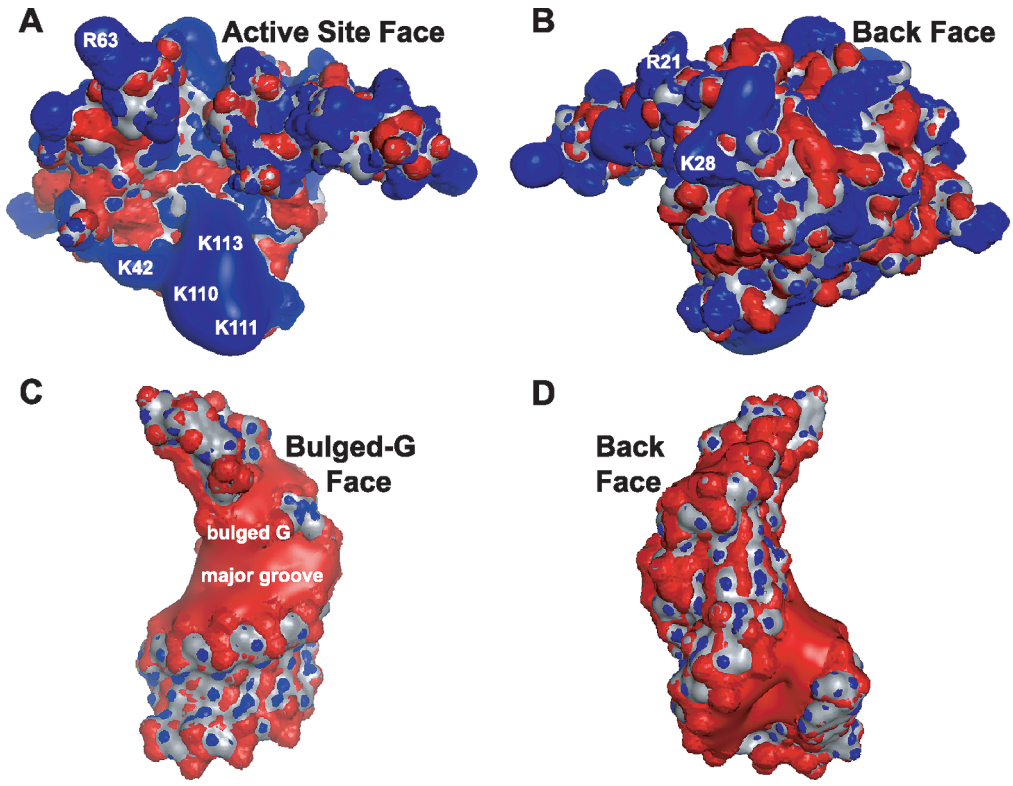

FIGURE 2: Isopotential contours mapped onto the surface of the substrate and enzyme. (A and B) Isopotential contours mapped onto the active site face (A) and back face (B) of restrictocin, using the molecular orientations from Figure 1D. Electrostatic potentials were calculated using APBS at 50 mM monovalent salt and displayed at 2.5 (blue) and −2.5 kT/e (red). (C and D) Isopotential contours mapped onto the bulged G face (C) and back face (D) of the SRL RNA; views are related by a 180° rotation. Electrostatic potentials were calculated using APBS at 50 mM monovalent salt and displayed at 7.5 (blue) and −7.5 kT/e (red).

3B). Importantly, the rank order of the change in salt dependence is the same for experimental and theoretical values. These results support the validity of these calculations and provide further evidence that the structures used provide a reasonable representation of the E:S complexes. In contrast, calculations do not agree with the experimental results for the noninterface R21D/K28D/K63D triple mutant; the Δn_{calc} is 3.0 for both structures, but the experimental Δn is 0.2 (*4*). Half of the Δn_{calc} for the triple mutant arises from removal of the three positive charges via alanine substitutions (data not shown); the remaining half arises from addition of negative charges at these positions. Perhaps the large change in net charge for this mutant (−6) alters the RNA−protein interactions in the ensemble of E:S complexes enough to negate the relevance of the crystal structures used for the calculations.

DISCUSSION

Cleavage of SRL RNA by restrictocin occurs in at least two kinetically distinct steps (*7*). First, an electrostatic complex (E:S) forms, which has little dependence on substrate sequence or structure over the entire range of salt concentrations used herein. The enzyme achieves cleavage specificity at the second k_2 step, meaning that features of the SRL contribute to transition-state stabilization. Presumably, E:S undergoes a conformational change prior to or at the transition state to allow the SRL-specific interactions with restrictocin. Electrostatic interactions between the positively charged restrictocin surface and the negatively charged SRL RNA substrate allow rapid formation of the E:S complex in a characteristically salt-dependent manner (*4, 7*). Restrictocin could form this E:S complex nonspecifically, with any subset of its basic surface residues contributing to RNA substrate binding. Alternatively, the complex could form specifically, with a distinct subset of restrictocin residues contributing to substrate binding.

Here, we demonstrate that restrictocin forms the E:S complex with the SRL RNA using a distinct subset of basic residues on its active site face (Figure 1). Mutation of cationic residues outside the putative interface does not affect the salt dependence of formation of the E:S complex, whereas mutation of cationic residues within the interface does. The lysine triad (K110, K111, and K113) makes the largest contributions to formation of the E:S complex, and these residues also make important contributions to catalysis (*27*). Consistent with these observations, in one cocrystal structure, these residues sit close to the enlarged major groove of the bulged G motif, which harbors dense negative charge arising from compaction of the phosphodiester backbone in a manner that resembles an S-turn. Perhaps the electrostatic attraction between the three lysines (the site of highest positive electrostatic potential on the protein surface) and the bulged G motif serves to localize the substrate at the active site for subsequent docking and cleavage. As a precedent for such an interaction, a related S-turn was shown to contribute electrostatically to RNA−protein binding (*23*).

The lysine triad near the active site likely contributes to formation of the restrictocin−ribosome E:S complex. Although we have not tested our mutants using ribosomes as substrates, binding of restrictocin to ribosomes shows an even stronger dependence on salt concentration than does binding of restrictocin to the SRL [$n = -9$ and −4, respectively

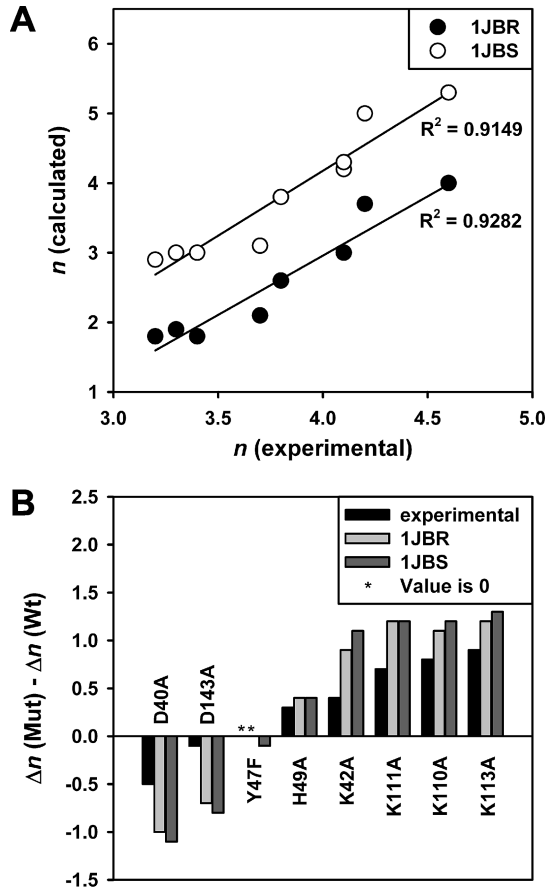

FIGURE 3: Comparison of experimental data with electrostatic calculations. (A) Correlation between experimental and calculated salt dependencies. The R^2 values shown are for linear regression fits to the data. (B) Comparison of theoretical and experimental salt dependence data. Calculated and experimental changes in salt dependence (Δn). Calculated values are shown for PDB entries 1JBR and 1JBS. Experimental values are listed in Table 1. The asterisks mark values for Y47F that are equal to zero and thus do not produce visible bars on the graph.

(*4*)], indicating a greater contribution from electrostatic interactions in the restrictocin−ribosome E:S complex. Consistent with the greater salt dependence, mutation of charged residues located outside the active site face affects ribosome binding but not SRL binding, implicating additional contacts with the ribosome or long-range tertiary interactions. Of the three mutations outside the active site face, the one lying closest to the SRL−restrictocin interface had the largest effect on the salt dependence for ribosome cleavage. However, mutation of residues close to the putative E:S interface has a larger effect on the salt dependence than mutation of residues farther from the interface, consistent with restrictocin binding in an oriented fashion to the ribosome.

Previously, the most extensive comparison of experimental and theoretical salt dependence for an RNA−protein interaction involved fragments of the phage λ N protein and its cognate RNA. That analysis used experimental data for only two point mutants (*28*). Building upon those previous studies, we have used the restrictocin−SRL system to obtain an expanded data set for comparison of theory with experiment. NLPB calculations are an accepted method for computing free energies of binding between nucleic acids and proteins. Our findings further demonstrate the usefulness of these calculations in predicting the contributions of residues to electrostatic interactions in RNA−protein complexes, even for RNA with a folded structure. In this report, we showed that each of the residues determined to contribute to formation of the E:S complex by experimental data was also identified by the NLPB calculations. Moreover, the calculations correctly identified the relative contribution of each mutant to formation of the E:S complex, from the smallest to the largest. Our computed Δn_{calc} values had little dependence on the solvent radius used, despite recent discussion of its possible significance (*29*). We used a solvent radius of 1.6 Å instead of a van der Waals surface because it reproduced more closely the experimental *n* values (data not shown). Given the paucity of studies of correlations between the experimental and theoretical changes in salt dependence upon removal of a surface charge, more study is warranted. However, our findings support electrostatic NLPB calculations as a powerful approach to identify residues that contribute to binding in electrostatic RNA−protein complexes.

Electrostatic interactions can facilitate macromolecular recognition by enhancing the collision frequency of the binding partners and by orienting the binding partners for subsequent short-range interactions. These mechanisms occur for protein−protein complexes. For example, barnase and barstar associate via initial formation of an electrostatic complex followed by formation of specific short-range interactions (*30*). We expect that many RNA binding proteins will exploit the polyanionic character of RNA to facilitate recognition via analogous electrostatic mechanism. For example, electrostatic interactions contribute to the binding of the U1A protein to the U1 hairpin II RNA, with basic residues enhancing RNA binding by increasing the rate of protein−RNA association (*31*). Our work demonstrates that restrictocin uses its basic residues on its active site face for substrate binding via electrostatic interactions, thereby enhancing catalytic efficiency.

ACKNOWLEDGMENT

We are grateful to Y.-L. Chan, J. Olvera, and I. G. Wool for valuable advice and discussion and to N. Gao for technical assistance.

REFERENCES

1. Record, M. T., Jr., Zhang, W., and Anderson, C. F. (1998) Analysis of effects of salts and uncharged solutes on protein and nucleic acid equilibria and processes: A practical guide to recognizing and interpreting polyelectrolyte effects, Hofmeister effects, and osmotic effects of salts. *Adv. Protein Chem. 51*, 281–353.
2. Park, C., and Raines, R. T. (2001) Quantitative analysis of the effect of salt concentration on enzymatic catalysis. *J. Am. Chem. Soc. 123*, 11472–11479.
3. Saecker, R. M., and Record, M. T. (2002) Protein surface salt bridges and paths for DNA wrapping. *Curr. Opin. Struct. Biol. 12*, 311–319.
4. Korennykh, A. V., Piccirilli, J. A., and Correll, C. C. (2006) The electrostatic character of the ribosomal surface enables extraordinarily rapid target location by ribotoxins. *Nat. Struct. Mol. Biol. 13*, 436–443.
5. Yang, X., and Moffat, K. (1996) Insights into specificity of cleavage and mechanism of cell entry from the crystal structure of the highly specific *Aspergillus* ribotoxin, restrictocin. *Structure 4*, 837–852.
6. Yang, X., Gerczei, T., Glover, L., and Correll, C. C. (2001) Crystal structures of restrictocin-inhibitor complexes with implications for RNA recognition and base flipping. *Nat. Struct. Biol. 8*, 968–973.
7. Korennykh, A. V., Plantinga, M. J., Correll, C. C., and Piccirilli, J. A. (2007) Linkage between Substrate Recognition and Catalysis

during Cleavage of Sarcin/Ricin Loop RNA by Restrictocin. *Biochemistry 46*, 12744–12756.
8. Wool, I. G. (1997) *Structure and Mechanism of Action of the Cytotoxic Ribonuclease* α*-Sarcin*, Academic Press, Inc., San Diego.
9. Lacadena, J., Alvarez-Garcia, E., Carreras-Sangra, N., Herrero-Galan, E., Alegre-Cebollada, J., Garcia-Ortega, L., Onaderra, M., Gavilanes, J. G., and Martinez Del Pozo, A. (2007) Fungal ribotoxins: Molecular dissection of a family of natural killers. *FEMS Microbiol. Rev. 31* (2), 212–237.
10. Olmo, N., Turnay, J., De Buitrago, G. G., De Silanes, I. L., Gavilanes, J. G., and Lizarbe, M. A. (2001) Cytotoxic mechanism of the ribotoxin α-sarcin Induction of cell death via apoptosis. *Eur. J. Biochem. 268*, 2113–2123.
11. Szewczak, A. A., and Moore, P. B. (1995) The sarcin/ricin loop, a modular RNA. *J. Mol. Biol. 247*, 81–98.
12. Szewczak, A. A., Moore, P. B., Chan, Y. L., and Wool, I. G. (1993) The conformation of the sarcin/ricin loop from 28S ribosomal RNA. *Proc. Natl. Acad. Sci. U.S.A. 90*, 9581–9585.
13. Correll, C. C., and Swinger, K. (2003) Common and distinctive features of GNRA tetraloops based on a GUAA tetraloop structure at 1.4 Å resolution. *RNA 9*, 355–363.
14. Correll, C. C., Beneken, J., Plantinga, M. J., Lubbers, M., and Chan, Y. L. (2003) The common and the distinctive features of the bulged-G motif based on a 1.04 Å resolution RNA structure. *Nucleic Acids Res. 31*, 6806–6818.
15. Gluck, A., and Wool, I. G. (1996) Determination of the 28 S ribosomal RNA identity element (G4319) for α-sarcin and the relationship of recognition to the selection of the catalytic site. *J. Mol. Biol. 256*, 838–848.
16. Endo, Y., Huber, P. W., and Wool, I. G. (1983) The ribonuclease activity of the cytotoxin α-sarcin. The characteristics of the enzymatic activity of α-sarcin with ribosomes and ribonucleic acids as substrates. *J. Biol. Chem. 258*, 2662–2667.
17. Baker, N. A., Sept, D., Joseph, S., Holst, M. J., and McCammon, J. A. (2001) Electrostatics of nanosystems: Application to microtubules and the ribosome. *Proc. Natl. Acad. Sci. U.S.A. 98*, 10037–10041.
18. Dolinsky, T. J., Nielsen, J. E., McCammon, J. A., and Baker, N. A. (2004) PDB2PQR: An automated pipeline for the setup of Poisson-Boltzmann electrostatics calculations. *Nucleic Acids Res. 32*, W665–W667.
19. Wang, J., Cieplak, P., and Kollman, P. A. (2000) How well does a restrained electrostatic potential (RESP) model perform in calculating conformational energies of organic and biological molecules? *J. Comput. Chem. 21*, 1049–1074.
20. Li, H., Robertson, A. D., and Jensen, J. H. (2005) Very fast empirical prediction and rationalization of protein pKa values. *Proteins 61*, 704–721.
21. Perez-Canadillas, J. M., Campos-Olivas, R., Lacadena, J., Martinez del Pozo, A., Gavilanes, J. G., Santoro, J., Rico, M., and Bruix, M. (1998) Characterization of pKa values and titration shifts in the cytotoxic ribonuclease α-sarcin by NMR. Relationship between electrostatic interactions, structure, and catalytic function. *Biochemistry 37*, 15865–15876.
22. Fisher, B. M., Ha, J. H., and Raines, R. T. (1998) Coulombic forces in protein-RNA interactions: Binding and cleavage by ribonuclease A and variants at Lys7, Arg10, and Lys66. *Biochemistry 37*, 12121–12132.
23. GuhaThakurta, D., and Draper, D. E. (2000) Contributions of basic residues to ribosomal protein L11 recognition of RNA. *J. Mol. Biol. 295*, 569–580.
24. Cunningham, B. C., and Wells, J. A. (1989) High-resolution epitope mapping of hGH-receptor interactions by alanine-scanning mutagenesis. *Science 244*, 1081–1085.
25. DeLano, W. L. (2002) Unraveling hot spots in binding interfaces: Progress and challenges. *Curr. Opin. Struct. Biol. 12*, 14–20.
26. Lacadena, J., Martinez del Pozo, A., Martinez-Ruiz, A., Perez-Canadillas, J. M., Bruix, M., Mancheno, J. M., Onaderra, M., and Gavilanes, J. G. (1999) Role of histidine-50, glutamic acid-96, and histidine-137 in the ribonucleolytic mechanism of the ribotoxin α-sarcin. *Proteins 37*, 474–484.
27. Plantinga, M. J. (2007) Ph.D. Thesis, The University of Chicago, Chicago.
28. Garcia-Garcia, C., and Draper, D. E. (2003) Electrostatic interactions in a peptide-RNA complex. *J. Mol. Biol. 331*, 75–88.
29. Qin, S., and Zhou, H. X. (2007) Do electrostatic interactions destabilize protein-nucleic acid binding? *Biopolymers 86*, 112–118.
30. Schreiber, G., and Fersht, A. R. (1996) Rapid, electrostatically assisted association of proteins. *Nat. Struct. Biol. 3*, 427–431.
31. Law, M. J., Linde, M. E., Chambers, E. J., Oubridge, C., Katsamba, P. S., Nilsson, L., Haworth, I. S., and Laird-Offringa, I. A. (2006) The role of positively charged amino acids and electrostatic interactions in the complex of U1A protein and U1 hairpin II RNA. *Nucleic Acids Res. 34*, 275–285.

BI800592G